environmental microbiology

Environmental Microbiology (2018) **20**(7), 2598–2614 doi:10.1111/1462-2920.14285

Bloom of a denitrifying methanotroph, '*Candidatus* Methylomirabilis limnetica', in a deep stratified lake

Jon S. Graf,[1]* Magdalena J. Mayr,[2,3] Hannah K. Marchant,[1] Daniela Tienken,[1] Philipp F. Hach,[1] Andreas Brand,[2,3] Carsten J. Schubert,[2] Marcel M. M. Kuypers[1] and Jana Milucka[1]

[1]*Max-Planck-Institute for Marine Microbiology, Department of Biogeochemistry, Bremen, Germany.*

[2]*Eawag, Surface Waters-Research and Management, Kastanienbaum, Switzerland.*

[3]*ETH Zurich, Institute of Biogeochemistry and Pollutant Dynamics, Zürich, Switzerland.*

Summary

Methanotrophic bacteria represent an important biological filter regulating methane emissions into the atmosphere. Planktonic methanotrophic communities in freshwater lakes are typically dominated by aerobic gamma-proteobacteria, with a contribution from alpha-proteobacterial methanotrophs and the NC10 bacteria. The NC10 clade encompasses methanotrophs related to '*Candidatus* Methylomirabilis oxyfera', which oxidize methane using a unique pathway of denitrification that tentatively produces N_2 and O_2 from nitric oxide (NO). Here, we describe a new species of the NC10 clade, '*Ca.* Methylomirabilis limnetica', which dominated the planktonic microbial community in the anoxic depths of the deep stratified Lake Zug in two consecutive years, comprising up to 27% of the total bacterial population. Gene transcripts assigned to '*Ca.* M. limnetica' constituted up to one third of all metatranscriptomic sequences *in situ.* The reconstructed genome encoded a complete pathway for methane oxidation, and an incomplete denitrification pathway, including two putative nitric oxide dismutase genes. The genome of '*Ca.* M. limnetica' exhibited features possibly related to genome streamlining (i.e. less redundancy of key metabolic genes) and adaptation to its planktonic habitat (i.e. gas vesicle genes). We speculate that '*Ca.* M. limnetica' temporarily bloomed in the lake during non-steady-state conditions suggesting a niche for NC10 bacteria in the lacustrine methane and nitrogen cycle.

Introduction

Temperate lakes are environments with intense methane cycling. Methane, a potent greenhouse gas, is abundantly produced in lake sediments from buried organic matter. Due to the comparably low sulfate concentrations, sulfate-dependent anaerobic methane oxidation often fails to completely consume the upward methane flux, in contrast to marine sediments. Therefore, large amounts of methane tend to enter the bottom waters of lakes. Lakes with oxic water columns, in which aerobic methane oxidation is constrained to a thin layer at the sediment surface, significantly contribute to atmospheric methane emissions (Bastviken *et al*., 2004). In contrast, methane is often completely consumed at the lake oxycline by aerobic methane oxidation in lakes that develop hypoxic and anoxic bottom waters.

Aerobic methane-oxidizing bacteria have long been recognized to play an important role in the regulation of methane emissions to the atmosphere (Oremland and Culbertson, 1992; Reeburgh, 2003). Major taxa of gammaproteobacterial methane-oxidizing bacteria (gamma-MOB) in lakes and other aquatic habitats include *Methylomonas, Methylobacter, Methylosoma* and *Methylosarcina* (Bowman, 2006). It has emerged recently that some of the gamma-MOB also thrive in apparently anoxic waters and sediments, where their activity can be sustained by oxygen production and transport (Blees *et al*., 2014; Milucka *et al*., 2015; Oswald *et al*., 2016), fermentation (Kalyuzhnaya *et al*., 2013) or denitrification (Kits *et al*., 2015a, 2015b; Oswald *et al*., 2017; Padilla *et al*., 2017). Interestingly, dedicated anaerobic methane oxidizers belonging or related to the ANME archaea (Knittel and Boetius, 2009; Haroon *et al*., 2013; Ettwig *et al*., 2016) seem to be constrained to lake sediments (Schubert *et al*., 2011; Weber *et al*., 2017) and play a comparably minor role in methane removal even in fully anoxic water columns.

Received 15 November, 2017; revised 3 April, 2018; accepted 4 April, 2018. *For correspondence. E-mail jgraf@mpi-bremen.de; Tel. +49-421-2028-653; Fax: +49-421-2028-690.

A group of methanotrophs, whose role in the environmental methane cycle is yet to be fully assessed, are the bacteria of the NC10 phylum (Raghoebarsing *et al*., 2006). These organisms oxidize methane using nitrite as an electron acceptor. The first described representative of this clade, '*Candidatus* Methylomirabilis oxyfera' has been proposed to have a unique capacity to disproportionate nitric oxide intracellularly and produce molecular oxygen, which is used for methane oxidation (Ettwig *et al*., 2010; Ettwig *et al*., 2012). This unique pathway allows NC10 to thrive in oxygen-depleted habitats, despite the obligate need for oxygen to activate and oxidize methane (Raghoebarsing *et al*., 2006; López-Archilla *et al*., 2007; Zhu *et al*., 2012; He *et al*., 2016; Padilla *et al*., 2016; Shen *et al*., 2016). Recent studies have demonstrated that NC10-related methanotrophs are present in the anoxic water column of a freshwater reservoir and sediments of deep freshwater lakes such as Lake Constance (Deutzmann and Schink, 2011; Deutzmann *et al*., 2014) and Lake Biwa (Kojima *et al*., 2012). They were proposed to significantly contribute to methane removal in these lakes even though direct activity of NC10 *in situ* has not been demonstrated to date and '*Ca.* M. oxyfera' rarely dominates bacterial, or specifically methanotrophic communities, particularly in planktonic habitats.

So far, bacteria of the NC10 phylum have not been found in Lake Zug (Oswald *et al*., 2016) or the other well-studied temperate lakes of Switzerland. Here, we report the finding of a '*Ca.* M. oxyfera'-related bacterium that dominated the bacterial community in the deep anoxic methane-rich hypolimnion in two consecutive years. We give a genomic description of this new putative species '*Candidatus* Methylomirabilis limnetica', infer its *in situ* activity from metatranscriptomics and describe the biogeochemical conditions during the sampling period that presumably led to the bloom of this bacterium.

Results and discussion

Biogeochemistry of Lake Zug

Lake Zug is a deep eutrophic freshwater lake located in Central Switzerland. The lake is permanently stratified and has reportedly not turned over since 1950 (Müller, 1993). During the sampling campaign in September 2016, several interesting features in the chemical profiles were noted (Fig. 1A and B).

The oxycline was located at about 106 m depth, well above the usual depth (140–150 m) that was measured in 2012, 2013 and 2014 (Oswald *et al*., 2016). No oxygen was detected with the trace optode (detection limit approximately 20 nmol l^{-1}) below this depth on two consecutive sampling days. In comparison to the years before (2012–2014, Oswald *et al*., 2016), methane concentrations at the given depths were ca. twofold higher and methane was depleted ca. 10 m below and not directly at the oxycline. During the sampling campaign in 2016, the flux of oxygen and methane across their respective zones of consumption was 7.8 and 2.2 mmol m^{-2} d^{-1}, respectively, and thus lower than the years before. Most interestingly, the concentration profile of NO_x (nitrate + nitrite) was concave, decreasing from ca. 22 μmol l^{-1} at the oxycline to a minimum of ca. 6 μmol l^{-1} at 150 m depth and then increasing again to a maximum of ca. 45 μmol l^{-1} at 180 m depth, as opposed to decreasing towards the sediment in the previous years (Oswald *et al*., 2016). Ammonium concentrations in the bottom waters were ca. threefold higher than in previous years and ammonium disappeared at ca. 115 m, the same depth where methane disappeared (Fig. 1B and Supporting Information Figure 1b). The flux of ammonium into this zone was 1.8 mmol m^{-2} d^{-1}. The profiles of both methane and ammonium indicated an additional zone of consumption between 150 and 160 m. The flux of methane and ammonium in the deeper depths was 2.6 and 4.9 mmol m^{-2} d^{-1} respectively.

We speculate that higher deposition rates of organic matter into the hypolimnion (through higher primary productivity or enhanced transport) resulted in a concomitant upward shift of the oxycline. This might have resulted in increased fluxes of methane and ammonium out of the sediment. The most parsimonious explanation for the obviously non-steady state NO_x profile is that, prior to our sampling campaign, vertical mixing or inflow of oxygen-rich, high density water (hyperpycnal flow) resulted in oxygen intrusion into the bottom waters, which in turn led to the oxidation of ammonium and production of nitrogen oxides.

The biogeochemical profiles recorded during a sampling campaign in October 2015 were more similar to the profiles described previously (Oswald *et al*., 2016). Oxygen was fully consumed at ca. 124 m depth, coinciding with the depletion of methane and ammonium (Supporting Information Figure 1a,b). NO_x concentrations decreased starting from 21 μmol l^{-1} at 118 m to 11 μmol l^{-1} at 140 m, the deepest depth measured in 2015 (Supporting Information Figure 1b). Between 122 m and 128 m nitrite was detected at low nanomolar concentrations but was otherwise below detection limit.

NC10 bacteria were abundant in the profundal anoxic waters of Lake Zug

In previous years, a large portion of upwards-diffusing methane was shown to be oxidized near the oxycline by abundant gamma-proteobacterial methane-oxidizing bacteria (Oswald *et al*., 2016). Additionally, it was shown that filamentous gamma-proteobacterial *Crenothrix* bacteria

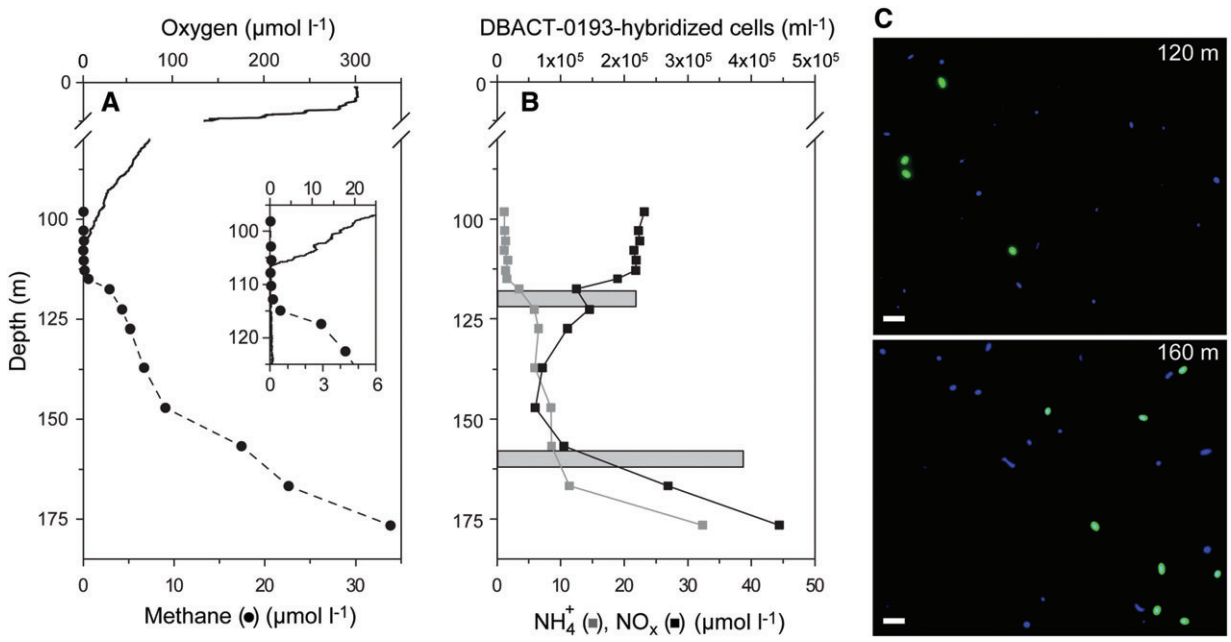

Fig. 1. Physico-chemical parameters and abundance of NC10 bacteria in Lake Zug in September 2016. A. Depth concentration profiles of oxygen and methane throughout the water column (100–180 m). The inset shows oxygen and methane concentration profiles near the oxycline. B. Concentration profiles of NO_x (nitrate + nitrite) and ammonium. The grey bars at 120 m and 160 m show absolute cell counts of NC10 bacteria identified by CARD-FISH (probe DBACT-0193). C. Fluorescent image of water from 120 m and 160 m showing NC10 bacteria (in green; counterstained with DAPI in blue) after CARD-FISH using a specific oligonucleotide probe DBACT-0193 (Supporting Information Table 1; Raghoebarsing *et al*., 2006). The scale bar represents 2.5 µm.

were major methane consumers in Lake Zug (Oswald *et al*., 2017).

To obtain a quantitative overview of the methane-oxidizing community in Lake Zug in 2016, we first classified and quantified 16S rRNA gene sequences in the unassembled metagenomic sequences from all three depths; near the oxycline (110 m), below it (120 m) and in the middle of the anoxic hypolimnion (160 m; Fig. 1A). For all three depths, a metagenome (Illumina HiSeq2500 2 × 250 bp) and a metatranscriptome (Illumina HiSeq3000 1 × 150 bp) were generated (Supporting Information Table 2). *Methylococcales* were stable members of the microbial community at all three investigated depths. Up to 10% of all 16S rRNA gene sequences were classified as *Methylococcales*; the majority of these belonged to genera *Methylobacter, Crenothrix, Methylomicrobium* and the CABC2E06 clade. Sequences classified as verrucomicrobial methanotrophs (mainly '*Ca.* Methylacidiphilum') were also detected, albeit at low abundance (0.1%–0.3%). Although verrucomicrobial methanotrophs related to '*Ca.* Methylacidiphilum' are known to thrive under thermoacidophilic conditions (Op den Camp *et al*., 2009), several studies have now detected '*Ca.* Methylacidiphilum'-related bacteria in more 'conventional' habitats (i.e. paddy soils, lake sediments; Sinclair *et al*., 2017; Vaksmaa *et al*., 2017). Known alphaproteobacterial methanotrophs (e.g., *Methylocystaceae* and *Beijerinckiaceae*) were not detected. This is consistent with the proteobacterial methanotrophic community analysed in this lake previously by catalysed reporter deposition fluorescence *in situ* hybridization (CARD-FISH; Oswald *et al*., 2016, 2017).

Interestingly, in the metagenomic sequences from 120 m and 160 m depth we found conspicuously high abundances of 16S rRNA gene sequences putatively assigned to the NC10 phylum. In these metagenomes, NC10-related sequences constituted approximately 10% and 19% of all classified metagenomic 16S rRNA gene sequences, respectively, and thus were up to two-fold more abundant than gamma-proteobacterial methanotrophs. At 110 m depth, which was nearest to the oxycline, only 0.7% of all classified 16S rRNA gene sequences were assigned to NC10. Somewhat lower abundances of NC10 were detected in Lake Zug in 2015, when NC10 abundance detected by 16S rRNA gene amplicon sequencing increased with depth to approximately 7% of all 16S rRNA gene sequences at 136 m depth (Supporting Information Figure 1b).

The high abundance of NC10 bacteria in 2016 was also confirmed by CARD-FISH (Fig. 1C). Water samples obtained from 120 m and 160 m were hybridized with an oligonucleotide CARD-FISH probe specific for NC10 bacteria (DBACT-0193). The samples contained 2.2 and 3.9×10^5 hybridized cells ml^{-1}, accounting for 10.0% (120 m) and 26.8% (160 m) of all DAPI-stained cells.

The DBACT-0193 probe has 1 nucleotide mismatch to the assembled 16S rRNA gene sequence belonging to NC10 retrieved from Lake Zug (Supporting Information Table 1). A similarly high proportion of cells was hybridized with the DBACT-1027 probe (0 mismatches; data not shown), whereas no hybridized cells were found with the DBACT-447 probe (5 mismatches).

Our CARD-FISH and metagenomic analyses showed that planktonic NC10 bacteria were the dominant methanotrophic microorganisms in the profundal, anoxic waters of Lake Zug in two consecutive years. To our knowledge, the abundance of NC10 found in 2016 is the highest relative abundance of NC10 that has been so far reported from any environment. The highest previous report was from the Feitsui reservoir where up to 16% of all cells were identified as NC10 using CARD-FISH (DBACT-1027 probe; Kojima *et al*., 2014). Interestingly, apart from being eutrophic, Lake Zug and Feitsui reservoir share few similarities. Whereas Lake Zug is a deep and permanently stratified temperate lake, Feitsui reservoir is a comparably shallow (mean depth of 40 m) and monomictic subtropical reservoir. It is thus not immediately obvious which conditions might favour the growth of NC10 to such high abundances.

One possible explanation for the high abundance of NC10 might be a transient formation of nitrite in the anoxic bottom waters that could have then subsequently stimulated growth of NC10 bacteria and lead to the observed bloom. For example, nitrite could have been formed by: (i) ammonium-oxidizing microorganisms after intrusion of oxygenated water into the ammonium-rich bottom waters (as indicated by the unusual NO_x profile) or by (ii) nitrate-reducing microorganisms reducing nitrate to nitrite. Several taxa which are known to contain denitrifying bacteria, such as *Methylococcaceae, Methylophilaceae* and *Comamonadaceae* were indeed found in the metagenomes from all three depths. The '*Ca.* Methanoperedens'-like archaea which have been repeatedly observed to co-occur with NC10 in bioreactor enrichment cultures (Raghoebarsing *et al*., 2006; Haroon *et al*., 2013; Ettwig *et al*., 2016) were not detected in our metagenomes. Intriguingly, sequences assigned to known ammonium-oxidizing genera such as '*Ca.* Nitrosoarchaeum' and '*Ca.* Nitrosopumilus' were detected even in the 'anoxic' metagenome from 160 m (1.2% of all 16S rRNA gene sequence, data not shown), which might indicate a past oxygenation event. In any case, the high abundance of NC10 bacteria in Lake Zug also suggests that these microorganisms were able to successfully compete for nitrite with anaerobic ammonium-oxidizing anammox bacteria, which were also detected in our Lake Zug metagenomes and are generally assumed to outcompete NC10 when ammonium is not limiting (Luesken *et al*., 2011a; Haroon *et al*., 2013). Anammox bacteria (*Ca.* Brocadia) were detected in all three investigated depths at abundances of ca. 0.1% – 0.6% of the total bacterial community *in situ.*

Genome reconstruction and phylogenetic assignment of 'Ca. M. limnetica'

The high abundance of NC10 bacteria in the samples enabled us to assemble a putative NC10 genomic bin. The binning process was based on guanine-cytosine content as well as differential contig coverage between metagenomes from 120 m and 160 m. A putative NC10 genomic bin was obtained from a co-assembly of all three depths. The contigs within this bin had the highest average coverage in the metagenomes from 120 m and 160 m (average contig coverage 451-fold and 851-fold) but only comparatively low coverage (30-fold) in the 110 m metagenome. The average contig coverage of the metagenomic bin matched well with the abundance of NC10 bacteria previously estimated in our 16S rRNA read survey and CARD-FISH analysis. Furthermore, we could not retrieve any other genomic bin related to '*Ca*. Methylomirabilis' from the co-assembled metagenomes from all three depths suggesting that only one dominant '*Ca.* Methylomirabilis' strain was present at all three depths. Summary statistics of the genomic bin (after targeted re-assembly) and comparison to the closed genome of '*Ca.* M. oxyfera' is shown in Supporting Information Table 3. Analysis by CheckM (Parks *et al*., 2015) suggested that the genomic bin was of high quality with similar estimates of completeness (96.2%) and contamination (1.7%) as the closed genome of '*Ca.* M. oxyfera' (accession FP565575.1, Supporting Information Table 3). Furthermore, analysis of the genomic bin by CheckM did not indicate strain heterogeneity.

Next we used the assembled full-length 16S rRNA gene sequence (1549 bp) retrieved from the NC10 genomic bin for taxonomic classification. Comparative analysis of the 16S rRNA gene sequence showed 95.1% identity to '*Ca.* M. sinica' (He *et al*., 2016) and 96.3% identity to '*Ca.* M. oxyfera' (Raghoebarsing *et al*., 2006; Ettwig *et al*., 2010). These values are higher than the threshold for genus definition (95%) but are below the species cutoff value (98.6%; Yarza *et al*., 2014; Konstantinidis *et al*., 2017). A whole genome analysis further showed that the pairwise average nucleotide identity (ANI) between our retrieved NC10 genome and the genome of '*Ca.* M. oxyfera' was 81.8%. This is well below the accepted ANI species boundary (95%–96%; Goris *et al*., 2007; Richter and Rosselló-Móra, 2009). The V3–V4 region of the assembled 16S rRNA gene sequence was identical to the sequence of the dominant NC10 OTU (428 bp) identified by 16S rRNA gene amplicon sequencing from samples retrieved in 2015. Taken

together these data suggest that the NC10 population present in Lake Zug qualifies as a new species within the genus '*Ca.* Methylomirabilis', which we named '*Candidatus* Methylomirabilis limnetica' [lim.ne′ti.ca. N.L. fem. adj. *limnetica* pertaining to lakes].

Phylogenetic analysis of the 16S rRNA gene sequences showed that the sequence of '*Ca.* M. limnetica' clustered within a subgroup of NC10 (Fig. 2A). The sequences within this subgroup were nearly identical (>99% sequence identity) and likely represented the same species. Interestingly, the sequences were retrieved from geographically distant freshwater lakes (Lake Constance, Germany; Lake Biwa, Japan; Deutzmann and Schink, 2011; Kojima *et al*., 2012), the Feitsui freshwater reservoir (Taiwan; Kojima *et al*., 2014) and a minerotrophic peatland (Brunssummerheide, The Netherlands; Zhu *et al*., 2012). Both currently described species of the genus '*Ca.* Methylomirabilis', '*Ca.* M. oxyfera' and '*Ca.* M. sinica', clustered in a different, more divergent branch of the 16S rRNA gene tree (Fig. 2A).

Phylogenetic analysis of the '*Ca.* M. limnetica' particulate methane monooxygenase subunit A (PmoA, Fig. 2B) showed that the sequence clustered together with partial PmoA sequences assigned to NC10 which were retrieved from Lake Constance (Deutzmann and Schink, 2011). The partial Lake Constance sequences were almost identical to the PmoA sequence of '*Ca.* M. limnetica' (98.2%–99.3%; 61%–69% coverage). Partial PmoA sequences retrieved from Brunssummerheide (Zhu *et al*., 2012), Lake Biwa (Kojima *et al*., 2012) and Feitsui reservoir (Kojima *et al*., 2014) formed a separate but closely related sister clade (approximately 96%–97% identity). A third, more distantly related polyphyletic cluster mainly constituted PmoA sequences retrieved from a waste water treatment plant (Lieshout; Luesken *et al*., 2011b), a river sediment (Bhattacharjee *et al*., 2016) as well as '*Ca.* M. oxyfera' and '*Ca.* M. sinica'. The sequences in this cluster were more distantly related to '*Ca.* M. limnetica' PmoA sequence (91%–96% identity).

Genome-inferred central C1 and energy metabolism

The high-quality genome of '*Ca.* M. limnetica' allowed for reconstruction of pathways involved in carbon and energy metabolism (Fig. 3). '*Ca.* M. limnetica' encoded the pathway for complete aerobic oxidation of methane (Table 1), including particulate methane monooxygenase (pMMO; *pmoCAB*) and one Xox-type methanol dehydrogenase (MDH; *xoxFJG*). Genes encoding for soluble methane monooxygenase (sMMO) and MxaF-type methanol dehydrogenase were not encoded in '*Ca.* M. limnetica' genome. Downstream conversion of formaldehyde to formate could either proceed via tetrahydromethanopterin (H_4MPT)-dependent or tetrahydrofolate (H_4F)-dependent C_1 transfer pathway. Formate dehydrogenase (*fdhA*), catalysing the oxidation of formate to CO_2, was also encoded in the genome of '*Ca.* M. limnetica'.

'*Ca.* M. limnetica' appears to derive its biomass carbon not from methane but solely from carbon dioxide, which has also been reported for '*Ca.* M. oxyfera' (Rasigraf *et al*., 2014). The genome encoded a complete Calvin-Benson-Bassham (CBB) cycle for autotrophic carbon fixation (Supporting Information Table 5) including ribulose-1,5-bisphosphate carboxylase/oxygenase (RubisCO; *cbbLS*) and phosphoribulokinase (*prk*), which are exclusive to the CBB cycle (Hügler and Sievert, 2011). Both the serine and ribulose monophosphate (RuMP) pathways of '*Ca.* M. limnetica', which allow for methane-derived carbon assimilation, were incomplete. The RuMP pathway was missing both key genes hexulosephosphate synthase (*hps*) and hexulosephosphate isomerase (*hpi*). The serine pathway was missing hydroxypyruvate reductase (*hpr*), glycerate 2-kinase (*gck*), malate thiokinase (*mtk*) and malyl-coenzyme A lyase (*mcl*).

Respiratory complexes of '*Ca.* M. limnetica'

It has been proposed that NC10 bacteria, specifically '*Ca.* M. oxyfera', produce O_2 from nitrogen oxides by a unique intra-aerobic denitrification pathway involving a nitrite reductase and a putative nitric oxide dismutase (Ettwig *et al*., 2010; Wu *et al*., 2011a; Ettwig *et al*., 2012). Also the genome of '*Ca.* M. limnetica' encoded for a partial denitrification pathway (Fig. 3; Table 1) including periplasmic nitrate reductase (*napAB*), cd_1-type nitrite reductase (*nirS*), two putative nitric oxide dismutases and one gene encoding for quinone-interacting nitric oxide reductase (qNOR; *norB*). Membrane-bound nitrate reductase (*narGHI*) and nitrous oxide reductase (*nosZ*) were not found in the '*Ca.* M. limnetica' genome. The amino-acid sequences of two putative nitric oxide dismutases of '*Ca.* M. limnetica' (encoded by tandem genes CLG94_00135 and CLG94_00140, Table 1) featured nearly all modified residues of the quinol-binding and catalytic site that have been identified in two putative nitric oxide dismutases of '*Ca.* M. oxyfera' and marine NC10 bacteria (Supporting Information Figure 5; Ettwig *et al*., 2012; Padilla *et al*., 2016). These putative nitric oxide dismutases, which are related to qNOR, have been suggested to catalyse the dismutation of two molecules of nitric oxide into N_2 and O_2 thus allowing NC10 bacteria to oxidize methane using pMMO in the absence of exogenous O_2 (Ettwig *et al*., 2010; Ettwig *et al*., 2012). Like '*Ca.* M. oxyfera', '*Ca.* M. limnetica' also encoded for a third, most likely genuine nitric oxide-reducing qNOR that contained the same

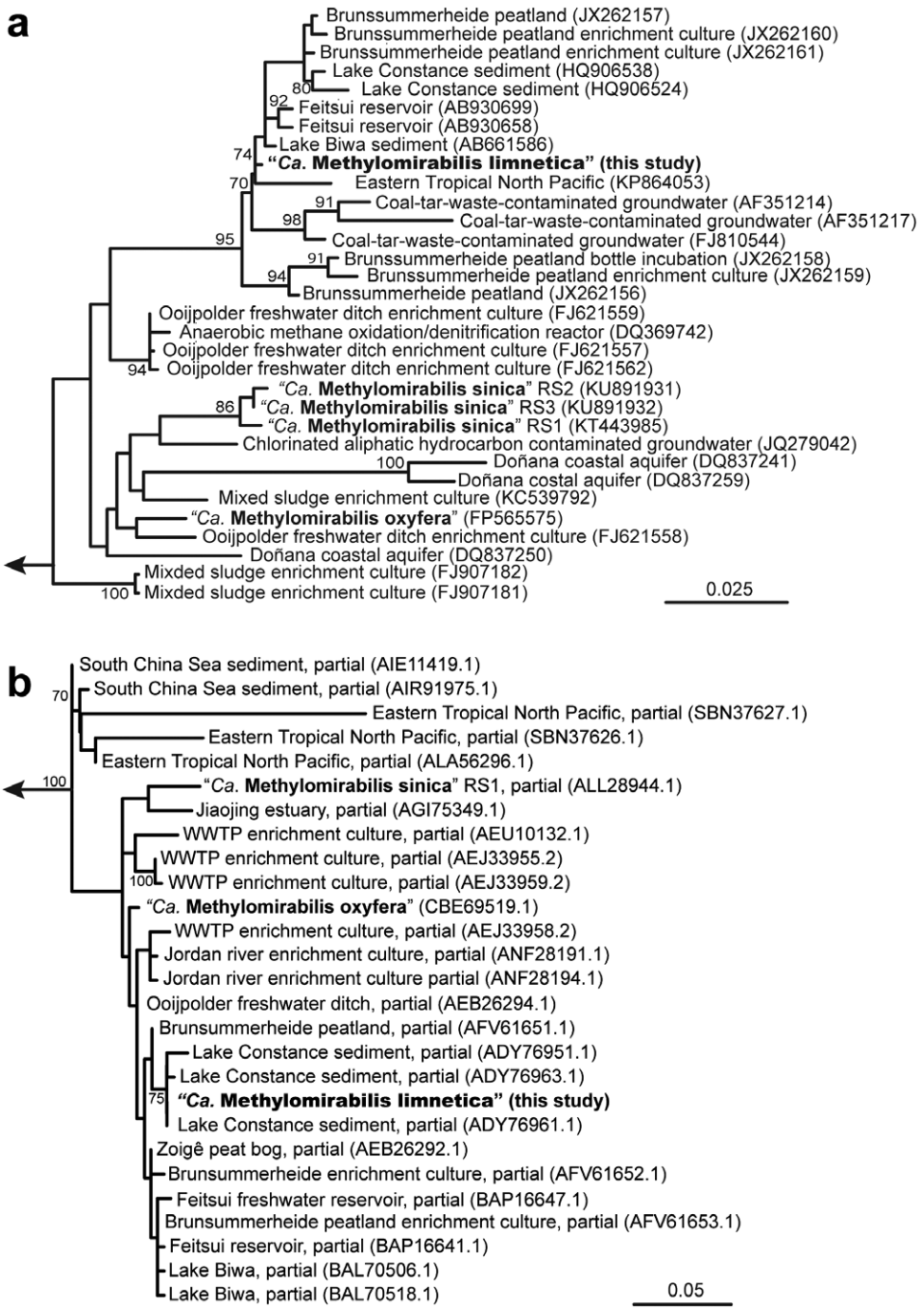

Fig. 2. Phylogenetic trees of '*Ca.* M. limnetica' full-length 16S rRNA gene (A) and PmoA amino-acid sequence (B). A. Maximum likelihood phylogenetic tree of 16S rRNA gene sequence without constraining the alignment by a weighting mask or filter. Bootstrap values >70% (out of 1000 resamplings) are shown in front of respective nodes. Three sequences of *Nitrospiraceae* were chosen as outgroup [*Leptospirillum ferriphilum* (AF356829), *Leptospirillum ferrooxidans* (X86776), *Nitrospira moscoviensis* (X82558)]. The scale bar indicates substitutions per site. B. Maximum likelihood phylogenetic tree of PmoA amino-acid sequence of '*Ca.* M. limnetica'. Bootstrap support (>70%) of total 500 resamplings is shown in front of respective nodes. Four PmoA/AmoA amino-acid sequences belonging to *Proteobacteria* and *Verrucomicrobia* served as outgroup (accession numbers BAE86885.1, AAG60667.1, CCJ08278.1, CCG92750.1). The scale bar indicates substitutions per site. Taxa names of described '*Ca.* Methylomirabilis' species are shown in bold.

conserved residues of canonical qNORs of '*Ca.* M. oxyfera' and other microorganisms (Supporting Information Figure 5).

In addition to nitrogen oxides, '*Ca.* M. limnetica' also has the genomic potential to use O_2 as terminal electron acceptor. We identified genes encoding for two types of terminal

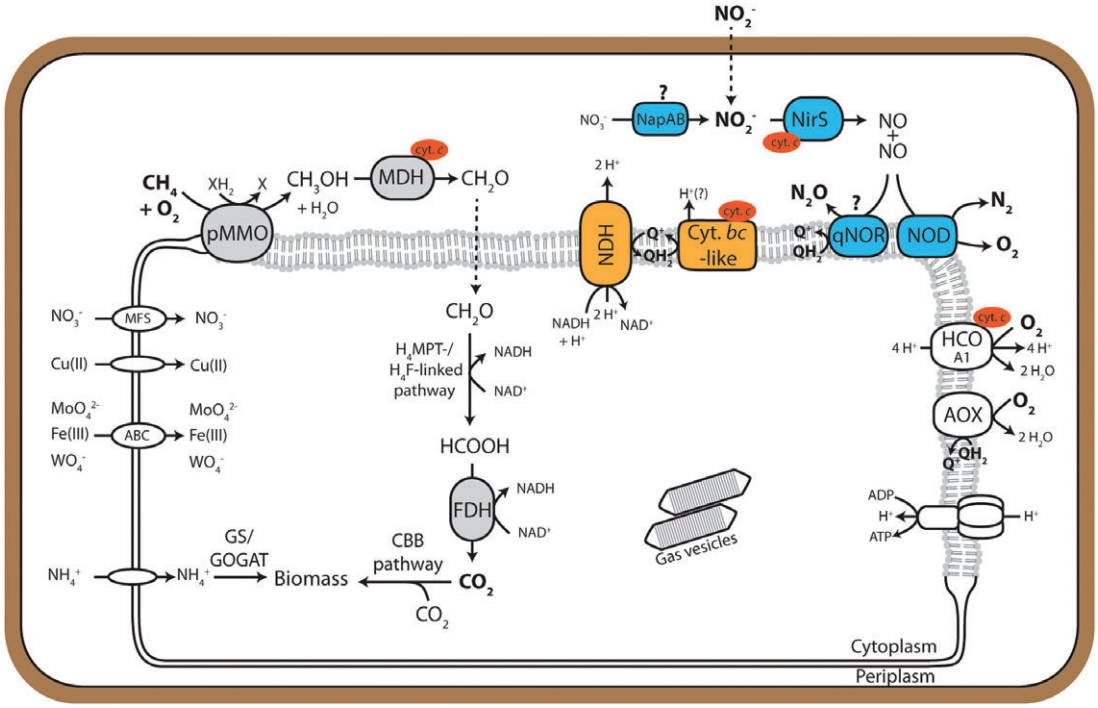

Fig. 3. Genome-inferred metabolic potential of '*Ca.* M. limnetica'. Predicted metabolic potential of '*Ca.* M. limnetica' with respect to carbon, nitrogen and respiratory pathways as well as selected transporters are shown.Indicated are the pathways for methane oxidation (grey), denitrification (blue) and (anaerobic) respiratory chain (orange). Abbreviations: pMMO, particulate methane monooxygenase; MDH, methanol dehydrogenase; FDH, formate dehydrogenase; CBB, Calvin-Benson-Bassham cycle; NapAB, periplasmic nitrate reductase; NirS, cytochrome cd_1 nitrite reductase; qNOR, quinol-dependent nitric oxide reductase; NOD, putative nitric oxide dismutase; cyt. *bc*-like, cytochrome *bc*-like complex; NDH, NADH dehydrogenase; AOX, alternative oxidase; HCO, heme-copper oxidase; GS/GOGAT, glutamine synthetase/glutamate synthase cycle; MFS, major facilitator superfamily; ABC, ATP-binding cassette transporter.

oxidases (Table 1); a heme copper oxidase (A1-type HCO; Pereira *et al*., 2001) and an alternative oxidase (AOX) that belongs to the di-iron carboxylate group of proteins (Berthold and Stenmark, 2003). Although NC10 bacteria grow anaerobically, it has been speculated that O_2 from nitric oxide dismutation could be respired by these terminal oxidases (Wu *et al*., 2011b). The genome of '*Ca.* M. oxyfera' also encoded for two additional heme-copper terminal oxidases (*bo*- and ba_3-type, labelled HCO 2 and 3; Wu *et al*., 2011b) which were however not found in the genome of '*Ca.* M. limnetica'. Alignment of Lake Zug metagenomic reads (160 m) to the genome of '*Ca.* M. oxyfera' further confirmed that these HCOs were encoded in genomic regions not present in our metagenomic dataset (Supporting Information Figure 3).

Intriguingly, several genes encoding for a cytochrome bc_1 complex, which have been identified in '*Ca.* M. oxyfera' (Ettwig *et al*., 2010; Wu *et al*., 2011b), were not found in the genome of '*Ca.* M. limnetica'. Instead we identified genes encoding for two cytochrome *bc*-like complexes, homologs of which were also encoded in the genome of '*Ca.* M. oxyfera' (Table 1). Both cytochrome *bc*-like complexes featured tandem genes encoding for a cytochrome *b* and a Rieske iron-sulfur protein in addition to multi-heme cytochromes *c* (Supporting Information Figure 4). The cytochromes *b* were either encoded as single, long gene (CLG94_00770) or as two separate, shorter genes (CLG94_01010–15) that appeared to constitute two different, evolutionary-related subfamilies of cytochromes *b* (Dibrova *et al*., 2013; Dibrova *et al*., 2017). As '*Ca.* M. limnetica' did not encode for a canonical cytochrome bc_1 complex, we suggest that either one or both cytochrome *bc*-like complexes, which were transcribed (Table 1), act as a quinol:cytochrome *c* oxidoreductase. The importance of Rieske/cytochrome *bc* complex for growth on nitrate and N_2O has recently been demonstrated in *Wolinella succinogenes* (Hein *et al*., 2017).

In addition to the cytochrome bc_1 complex, several other key metabolic genes encoding for nitrogen metabolism and the respiratory chain of '*Ca.* M. oxyfera' appeared to be absent from the genome of '*Ca.* M. limnetica' (Supporting Information Table 4). These were genes encoding for membrane-bound nitrate reductase (Nar), two heme copper oxidases (previously assigned HCO2 and HCO3; Wu *et al*., 2011b), MxaF-type as well as one additional XoxF-type methanol dehydrogenase and hydroxylamine oxidoreductase (Hao, also known as hydroxylamine dehydrogenase). The absence of *hao* genes from the '*Ca.* M. limnetica' genome is

Table 1. *In situ* transcription of functional genes involved in methane oxidation and respiration of '*Ca.* M. limnetica'. Listed are functional genes encoding for dissimilatory nitrogen metabolism and respiratory complexes of '*Ca.* M. limnetica' as well as genes encoding for the complete methane oxidation. Transcription was quantified as RPKM (reads per 1 kb gene length and per million mapped transcripts) in metatranscriptomes obtained from 110 m, 120 m and 160 m depth. Gene homologs of '*Ca.* M. oxyfera' (FP565575.1) have been identified using amino-acid sequences BLASTP; only the top hit (by *e*-value or % sequence identity) is shown (alignment coverage >93%; except NapA 83%).

				Transcription (RPKM)		
Protein	*Gene*	*Locus tag*	*Homolog 'Ca. M. oxyfera'*	110 m	120 m	160 m
Dissimilatory nitrogen metabolism and respiratory complexes						
Periplasmic nitrate reductase	napA	CLG94_12775	DAMO_2411	435	411	403
	napB	CLG94_12770	DAMO_2410	746	495	522
Nitrite reductase	nirS	CLG94_12790	DAMO_2415	7,485	15,646	16,160
Nitric oxide reductase	norZ1	CLG94_04925	DAMO_1889	478	240	227
Putative nitric oxide dismutase	-	CLG94_00140	DAMO_2434	12,188	82	89
Putative nitric oxide dismutase	-	CLG94_00135	DAMO_2437	40,540	31,626	33,264
Cytochrome c oxidase, A1-type	coxIIII	CLG94_02145	DAMO_1162	116	263	230
	coxIII	CLG94_02150	DAMO_1164	109	198	183
	coxI	CLG94_02155	DAMO_1165	113	129	129
	coxII	CLG94_02160	DAMO_1166	159	152	141
Alternative oxidase	aox	CLG94_05450	DAMO_2910	62	114	100
Cytochrome *bc*-like complex	qcrA	CLG94_00765	DAMO_0820	229	449	427
	qcrB	CLG94_00770	DAMO_0821	217	352	356
	-	CLG94_00775	DAMO_0822	191	327	327
Cytochrome *bc*-like complex	qcrA	CLG94_01010	DAMO_1672	431	301	258
	qcrB	CLG94_01015	DAMO_1671	402	301	299
	-	CLG94_01020	DAMO_1670	237	185	178
	-	CLG94_01025	DAMO_1669	311	323	317
Methane oxidation						
Particulate methane monooxygenase	pmoC	CLG94_00090	DAMO_2451	20,096	19,864	20,895
	pmoA	CLG94_00095	DAMO_2450	11,744	16,567	17,627
	pmoB	CLG94_00100	DAMO_2448	11,669	15,996	16,568
Methanol dehydrogenase	xoxG	CLG94_05355	DAMO_0138	736	1,174	1,089
	xoxJ	CLG94_05360	DAMO_0136	777	1,393	1,355
	xoxF	CLG94_05365	DAMO_0134	4,206	6,552	6,669
Formaldehyde activating enzyme	fae	CLG94_06605	DAMO_0454	4,534	8,344	7,400
Methylene H_4MPT dehydrogenase	mtd	CLG94_06610	DAMO_0455	1,298	2,694	2,645
Formyltransferase/hydrolase complex	fhcB	CLG94_06620	DAMO_0457	776	1,553	1,545
	fhcA	CLG94_06625	DAMO_0458	567	1,052	1,020
	fhcD	CLG94_06630	DAMO_0459	580	1,230	1,155
	fhcC	CLG94_06635	DAMO_0460	777	1,501	1,399
Bifunctional methylene H_4F dehydrogenase / methenyl H_4MPT cyclohydrolase	folD	CLG94_03935	DAMO_1852	322	391	336
Formyl H_4F deformylase	purU	CLG94_11150	DAMO_2586	69	58	65
Formate dehydrogenase	fdhA	CLG94_00865	DAMO_0853	130	194	207

intriguing as Hao has been suggested to play a role in the detoxification of hydroxylamine in methanotrophs (Nyerges and Stein, 2009; Campbell *et al*., 2011). Hydroxylamine is formed via the co-metabolism of ammonia by methane monooxygenase—a process that is likely also relevant in Lake Zug as methane and ammonium were present in almost equimolar concentrations *in situ* (Fig. 1A and B). Other genes encoding for enzymes known to be involved in hydroxylamine detoxification, such as cytochrome P460 (*cytL*; Bergmann *et al*., 1998), were also absent from the '*Ca.* M. limnetica' genome thus raising the question of how '*Ca.* M. limnetica' disposes of this toxic intermediate. Detoxification of potentially formed hydroxylamine could either be performed by '*Ca.* M. limnetica' periplasmically via a yet unidentified non-canonical hydroxylamine oxidoreductase or could alternatively involve hydroxylamine export and degradation by other members of the microbial community.

To confirm that genes known to mediate hydroxylamine detoxification (*hao, cytL*) in methanotrophs were indeed absent from the genome of '*Ca.* M. limnetica' we searched the whole metagenomic assembly for genes encoding the aforementioned enzymes but could not identify highly covered contigs encoding for close homologs. Additionally, by mapping the sequences of the 160 m metagenome to the genome of '*Ca.* M. oxyfera' we found that whereas genomic regions with gene homologs shared between both species were well covered (per-base coverage >100), the average coverage was close to zero for all genomic regions containing genes,

which included *hao*, that appear exclusive to '*Ca.* M. oxyfera' (Supporting Information Figure 3).

In situ gene transcription of '*Ca.* M. limnetica'

To investigate whether '*Ca.* M. limnetica' was transcriptionally active *in situ* during our sampling campaign in 2016, we aligned the metatranscriptomic reads obtained from 110 m, 120 m and 160 m depth to the '*Ca.* M. limnetica' genome. We found that nearly one third of all non-rRNA metatranscriptomic sequences from 120 m and 160 m (28.4% and 32% respectively) aligned to the genome of '*Ca.* M. limnetica'. The overall alignment rate of the metatranscriptome from 110 m (2.8%) was much lower, in line with the much lower abundance of '*Ca.* M. limnetica' at this depth. 16S rRNA amplicon sequencing of RNA samples obtained in 2015 also showed that NC10 bacteria were actively transcribing 16S rRNA genes. In water samples from 136 m and 140m, the relative abundance of 16S rRNA assigned to NC10 bacteria constituted approximately 22% of all 16S rRNA sequences.

A comparison of the 100 most transcribed genes of '*Ca.* M. limnetica' in our metatranscriptomic datasets from 2016 showed a clear difference between metatranscriptomes originating from near the oxycline (110 m) and from below (120 and 160 m). We found that 94 out of the top 100 transcribed genes were shared between the two metatranscriptomes from 120 m and 160 m depth. This was not the case for the 110 m metatranscriptome, where only about half of the top 100 transcribed genes were shared with the metatranscriptomes from 120 m and 160 m. We found several genes encoding for toxin-antitoxin systems and proteases exclusively transcribed among the top 100 genes by '*Ca.* M. limnetica' at 110 m. Toxin-antitoxin systems appear to have an important role in bacterial stress physiology and growth control (Buts *et al*., 2005; Hayes and Low, 2009; Blower *et al*., 2011). Hence, the increased transcription of these genes might reflect a response of '*Ca.* M. limnetica' to hypoxic conditions close to the oxycline.

Transcription of functional genes involved in methane oxidation and denitrification was in accord with the proposed anaerobic, methanotrophic and denitrifying lifestyle of NC10 bacteria. Among the 100 most transcribed genes of '*Ca.* M. limnetica' shared in all three metatranscriptomes were the genes encoding for methane oxidation and denitrification (Table 1); in particular genes encoding for particulate methane monooxygenase, nitrite reductase and one gene copy of the putative nitric oxide dismutase (CLG94_00135) were highly transcribed. At 120 m and 160 m, transcription of the second gene copy (CLG94_00140) was three orders of magnitude lower. Interestingly, at 110 m both putative nitric oxide dismutase genes were highly transcribed (Table 1). This observation is in line with the suggestion of Luesken and colleagues (2012) who proposed that '*Ca.* M. oxyfera' might only transcribe both copies of nitric oxide dismutase when exposed to oxygen. Transcription of the 'canonical' nitric oxide reductase was detected at all depths, implying that '*Ca.* M. limnetica' might also reduce nitric oxide to N_2O *in situ*. However, the transcription levels of the 'canonical' nitric oxide reductase were significantly lower than those of the predominantly transcribed putative nitric oxide dismutase (84 to 146-fold). '*Ca.* M. limnetica' also encoded a periplasmic nitrate reductase (NapAB) but its transcription was much lower than that of, for example, the nitrite reductase (NirS, Table 1). It thus remains unclear whether '*Ca.* M. limnetica' can use nitrate as an electron acceptor *in situ*. '*Ca.* M. oxyfera', which also possesses NapAB, was incapable of using nitrate as electron acceptor for methane oxidation (Ettwig *et al*., 2010).

Besides genes involved in methane oxidation and dissimilatory nitrogen metabolism, many genes encoding for proteins involved in transcription and translation (i.e. RNA polymerase, translation initiation factor) as well as numerous ribosomal proteins were among the highest transcribed genes at all depths. Furthermore, we identified a well transcribed gene cluster encoding for several gas vesicle-related proteins including the main structural gas vesicle protein (GvpA) and associated proteins (GvpL/F, GvpN and GvpK). In fact, one *gvpA* gene was among the highest transcribed genes at all depths (~30,000 RPKM at 120 m and 160 m). The presence and transcription of genes encoding for gas vesicles suggests that '*Ca.* M. limnetica' might be capable of adjusting or maintaining its position in the water column. Interestingly, '*Ca.* M. oxyfera', which was isolated from freshwater sediment, appears not to encode homologs of these Gvp-associated proteins.

Concluding remarks

'*Ca.* Methylomirabilis limnetica', a new species of the candidate genus *Methylomirabilis*, dominated the methanotrophic and even overall microbial community in the hypolimnion of a deep stratified lake. We speculate that high organic matter deposition and a possible oxygenation of the hypolimnion prior to the sampling campaign might have triggered the bloom of '*Ca.* M. limnetica'. The large proportion of highly transcribed genes in all three *in situ* transcriptomes suggests that at the time of sampling the '*Ca.* M. limnetica' population was still transcriptionally active, even though it is not clear whether this activity was accompanied by methane oxidation. Our phylogenetic analyses show that '*Ca.* M. limnetica' occurs in a variety of freshwater habitats and might possibly be adapted to a planktonic lifestyle, as suggested by the unique presence of gas vesicle-encoding genes in its genome.

Experimental procedures

Geochemical profiling and sample collection

Sampling was carried out in September 2016 and October 2015 at a single station located in the deep, southern lake basin of Lake Zug (~200 m water depth; 47°06′00.8″ N, 8°29′35.0″ E). A multi-parameter probe was used to measure conductivity, turbidity, depth (pressure), temperature and pH (XRX 620, RBR, Ottawa, ON, Canada). Dissolved oxygen was monitored online with normal and trace micro-optodes (types PSt1 and TOS7, Presens, Regensburg, Germany) with detection limits of 125 and 20 nM, respectively, and a response time of 7 s.

In 2016, water samples for measurements of methane and nitrous oxide concentrations were retrieved from distinct depths with a syringe sampler. Water from individual 50 ml syringes was filled through a gas-tight rubber tubing into serum bottles (120 ml), allowing water to overflow. Solid copper chloride ($CuCl_2$) was immediately added in excess to the water samples and the bottles were closed with a butyl rubber stopper (head-space free) and crimped. Before analysis, a 30 ml headspace was set with N_2 and after overnight equilibration methane and nitrous oxide concentrations were measured in the headspace. In 2015, 20 ml of lake water were taken for methane analysis with a syringe sampler and filled into closed 40 ml serum bottles containing 4g NaOH pellets and 600 mbar N_2 gas. The NaOH pellets were found to release methane, and this contamination was subtracted from the total methane measured in each sample. Headspace methane samples from 2016 and 2015 were measured with a gas chromatograph (Agilent 6890 N, Agilent Technologies, Santa Clara, CA, USA) equipped with a Carboxen 1010 column (30m × 0.53 mm, Supelco, Bellefonte, PA, USA) and a flame ionization detector. Methane concentrations in the water phase were back-calculated according to Wiesenburg and Guinasso (1979).

Concomitantly with dissolved gases, water samples for ammonium and NO_x measurements (only samples from 2016) were collected from the same depths using the same syringe sampler. Forty millilitre of water was directly injected into a 50 ml Falcon tube containing 10 ml of OPA reagent for fluorometric ammonium quantification according to Holmes and colleagues (1999). For NO_x quantification, 1.5 ml of water was added to an eppendorf cup prefilled with 15 µl $HgCl_2$ and combined nitrate and nitrite concentration was determined by commercial chemiluminescence NO_x analyser after reduction to nitric oxide with acidic Vanadium (II) chloride (Braman and Hendrix, 1989). After reduction to nitric oxide, nitrite was determined with acidic potassium iodide and nitrate was then calculated as the difference between NO_x and nitrite. For ammonium and NO_x analysis of samples collected in 2015, syringe samples were pre-filtered with a cellulose acetate filter (0.2 µm pore size). Ammonium was quantified according to Parsons and colleagues (1984) and nitrate and nitrite were measured by flow-injection analysis (FIA; SAN++, Skalar) following ISO 13395.

In 2016, samples were taken for CARD-FISH analysis. For that, 3 ml of water were sampled from 120 m and 160 m depth into a 15 ml Falcon tube containing 0.3 ml 20% formaldehyde.

In 2016, water for DNA/RNA analyses was collected with a Niskin bottle from 110 m, 120 m and 160 m water depth. For each depth, 2 × 1 L water was immediately filtered onboard (0.2 µm GTTP filter; Merck Millipore, Darmstadt, Germany); filters for DNA extraction were air dried and filters for RNA extraction were immediately immersed in RNAlater preservation solution (Life Technologies, Carlsbad, CA, USA). DNA and RNA filters were stored at –20°C until further processing. In 2015, 105–220 ml water for DNA/RNA analyses were collected with a syringe sampler, immediately filtered on board onto a 0.2 µm pore size cellulose acetate filter (Sartorius, Göttingen, Germany) and immediately frozen on dry ice and stored at –80°C until further processing.

Diffusive flux calculation

Diffusive fluxes (J) of oxygen, ammonium and methane were calculated assuming steady state using Fick's first law:

$$J = -D\frac{\partial C}{\partial z},$$

where $\partial C/\partial z$ is the concentration gradient. Following Oswald and colleagues (2016), we used a turbulent diffusion coefficient D of 2.7×10^{-5} m^2 s^{-1}. This value was determined in Lake Zug by the heat budget method (Powell and Jassby, 1974) using temperature data from September 2012 to June 2013. In order to calculate fluxes towards the chemocline, a depth interval between 60 and 106 m was used for O_2 and a depth interval between 120 and 117.5 m for CH_4 and NH_4^+. CH_4 and NH_4^+ flux in deeper depths was calculated over a depth interval between 150 and 180 m and 170 and 180 m respectively.

Catalysed reporter deposition-fluorescence in situ hybridization (CARD-FISH)

Waters samples (3 ml) were fixed with formaldehyde (final concentration 2% [w/v]) for up to 12 h at 4°C before being filtered onto polycarbonate GTTP filters (0.2 µm pore size, effective filter diameter = 20 mm; Merck Millipore, Darmstadt, Germany). Permeabilization with lysozyme, peroxidase

inactivation, hybridization with specific oligonucleotide probes labelled with horseradish peroxidase (for details see Supporting Information Table 1; Biomers, Ulm, Germany), tyramide reporter deposition (Oregon Green 488) and 4′,6-diamidino-2-phenylindole (DAPI) counter staining was performed according to Pernthaler and colleagues (2002). Filters were embedded in a mix of Citifluor/Vectashield (4:1) and mounted onto glass slides. Cell counting was performed with a Eclipse Ci microscope (Nikon Instruments, Germany) in randomly selected fields of view until ~1,000 DAPI-stained cells were counted.

Nucleic acid extraction, 16S rRNA (gene) sequencing and whole metagenome and metatranscriptome sequencing

For nucleic acid extraction from samples collected in 2015, DNA and RNA were extracted simultaneously with the AllPrep DNA/RNA Mini Kit (Qiagen). Residual DNA in the RNA extract was digested with TURBO DNA-free kit (Invitrogen).

For samples collected in 2016, DNA was extracted from cut-up filters using Powersoil DNA isolation kit. For RNA extraction, filters were briefly rinsed with nuclease-free water and RNA was extracted from cut-up filters using PowerWater RNA isolation kit (including removal of genomic DNA by DNase I digestion). Both nucleic acid extraction kits (MoBio Laboratories, Carlsbad, CA, USA) were used according to manufacturer's instructions. DNA and RNA were quantified using the Qubit dsDNA HS or RNA HS Assay kits and the Qubit 2.0 Fluorometer (Invitrogen, Carlsbad, CA, USA).

For metagenomic sequencing, DNA was fragmented by sonication (500 nt) using a Covaris S2 sonicator (Covaris, Woburn, MA, USA) and library preparation was done according to manufacturer's instructions using NEBNext Ultra II DNA Library Prep Kit for Illumina (New England Biolabs, Ipswich, MA, USA). Paired-end sequencing (2 × 250 bp) was performed using the Illumina HiSeq2500 platform (Illumina, San Diego, CA, USA) in rapid mode with SBS chemistry v2.

For metatranscriptomic sequencing, total RNA was first concentrated using the RNA Clean and Concentrator kit (Zymo Research Corp., Irvine, CA, USA) according to manufacturer's instructions. Depletion of rRNAs was done with the Ribo-Zero rRNA Removal Kit (Bacteria) for Illumina (Epicentre, Madison, WI, USA) with a protocol adaptation for low input amounts. cDNA library preparation was done with the NEBNext Ultra Directional RNA Library Prep Kit for Illumina (New England Biolabs) according to protocol and sequencing (1 × 150 bp) was performed using the Illumina HiSeq3000 platform (Illumina) with SBS chemistry. Library preparation and sequencing was performed by the Max Planck-Genome-centre Cologne, Germany (http://mpgc.mpipz.mpg.de/home/). Detailed information for each metagenomic and metatranscriptomic dataset can be found in Supporting Information Table 2.

For 16S rRNA (gene) sequencing (only 2015 samples), RNA was reverse-transcribed with random hexamers into cDNA with SuperScript™ IV First-Strand Synthesis System (Invitrogen). The library preparation of 16S rRNA and rDNA for Illumina MiSeq sequencing was done with a two-step PCR using NEBNext Q5® Hot Start HiFi PCR Master Mix (New England Biolabs). The first PCR (17 cycles, initial denaturation 30 s, 98°C, denaturation 10 s, 98°C, annealing 35 s, 54°C, extension 35 s, 65°C and final extension 5 min, 65°C) was done in triplicates with tailed forward primer S-D-Bact-0341-b-S-17 and tailed reverse primer S-D-Bact-0785-a-A-21 (Klindworth *et al*., 2013). The products were pooled and cleaned with Agencourt AMPure XP kit (BeckmanCoulter, Brea, CA, USA) followed by a second PCR (8 cycles, annealing at 55°C) to attach Illumina barcodes and adapters using Nextera XT Index Kit set A and D (Illumina). Libraries were cleaned again, quantified by fluorometry with Qubit DNA BR reagents (Invitrogen) and measured on a microplate reader (Spark M10; Tecan, Männedorf, Switzerland). Libraries were pooled and quality was controlled with Tape Station 2200 (Agilent). Sequencing was performed using the Illumina MiSeq platform (Illumina) with 600-cycle MiSeq reagent kit v3 (Illumina) and 10% PhiX. Amplicon sequencing was done at the Genetic Diversity Centre (GDC) of ETH Zurich.

Metagenomic assembly, binning and genome analysis

Paired-end Illumina reads were trimmed using Trimmomatic 0.32 (Bolger *et al*., 2014) and parameters MINLEN:20 ILLUMINACLIP: TruSeq3-PE.fa:2:30:10 LEADING:3 TRAILING:3 SLIDINGWINDOW:4:15 MINLEN:50. Trimmed Illumina reads from all three metagenomes were co-assembled using metaSPAdes assembler 3.9.1 (Nurk *et al*., 2017) and k-mer lengths of 21,33,55,77,99,127. Illumina reads of each metagenome were mapped to the assembled contigs using BBmap 35.43 (Bushnell, 2016) with approximate minimum identity of 95% (minid = 0.95) and default parameters. Open reading frames were predicted using Prodigal 2.60 (Hyatt *et al*., 2010) running in metagenomic mode (-p meta) and standard parameters. Translated amino-acid sequences were subsequently searched for using HMMER3 (http://hmmer.org/) against a set of 107 hidden markov models of essential single-copy genes (Dupont *et al*., 2012) using trusted cutoff values (-cut_tc) and default settings. Protein sequences coding for essential single-copy genes were searched against NCBI non-redundant database (retrieved August 2015) using DIAMOND 0.8.34 blastp

(Buchfink *et al*., 2015) and an *e*-value cutoff of 10^{-6}. The taxonomy (class level) of each essential single-copy gene was assigned using MEGAN5 and the mmgenome script 'hmm.majority.vote.pl' (http://madsalbertsen.github.io/mmgenome/). Binning of '*Ca.* M. limnetica' contigs from the co-assembly was based on differential contig coverage in metagenomes from 160 m and 120 m (Supporting Information Figure 2) and was performed using the mmgenome R package [http://madsalbertsen.github.io/mmgenome/; (Karst *et al*., 2016)]. Trimmed Illumina reads of the 160 m metagenome were mapped to the binned contigs using BBmap and stringent mapping settings (approximate minimum identity = 0.95). Ten percent of the mapped reads were selected at random and re-assembled using SPAdes 3.50 (Bankevich *et al*., 2012) with mismatch corrector enabled (-careful). The re-assembly was further refined by removing short and low-coverage contigs (length < 500, average coverage < 10-fold). The quality of the re-assembled genome was assessed using CheckM 1.05 (Parks *et al*., 2015) running the lineage-specific workflow and genome annotation was performed using Prokka 1.12 (Seemann, 2014) in metagenomic mode (-metagenome) and the RAST online annotation server (Aziz *et al*., 2008). The annotation of key metabolic pathways was manually inspected and refined.

The Whole Genome Shotgun project of '*Ca.* Methylomirabilis limnetica' has been deposited at DDBJ/ENA/GenBank under the accession NVQC00000000 and BioProject PRJNA401219. The version described in this article is version NVQC01000000. Raw metatranscriptomic sequencing data has been deposited at the NCBI Sequence Read Archive under accession SRP132411 (SRR6684601, SRR6684602, SRR6684603).

For microbial community analysis from metagenomic Illumina reads, trimmed paired-end reads matching the 16S rRNA gene sequence were identified using SortMeRNA 2.1 (Kopylova *et al*., 2012) and archaeal and bacterial 16S rRNA databases (silva-arc-16S-id95, silva-bac-16S-id90). Paired-end rRNA gene sequences were then merged using BBmerge (Bushnell, 2016) with a minimum overlap of 20 bases. The merged reads (~8,700–11,400 sequences for each metagenome) were submitted to the SILVAngs web service (Quast *et al*., 2013) for taxonomic classification.

Pairwise average nucleotide identity (ANI) values between the genomes of '*Ca.* M. limnetica' and '*Ca.* M. oxyfera' were calculated using BLAST (ANIb) and the JSpeciesWS online service (Richter *et al*., 2016). Relative genome sequence coverage of '*Ca.* M. oxyfera' (Supporting Information Figure 3) was calculated by mapping trimmed metagenomic sequences from Lake Zug (160 m) to the genome of '*Ca.* M. oxyfera' (retrieved from GenBank; accession FP565575) using BBmap 35.43 (Bushnell, 2016) and standard settings. Average genome coverage (500 bp interval) was calculated and visualized using BLAST Ring Image Generator (Alikhan *et al*., 2011). Gene coordinates of selected genes were imported from GenBank and Refs. (Wu *et al*., 2011b; Luesken *et al*., 2012). Homologs shared between '*Ca.* M. limnetica' and '*Ca.* M. oxyfera' were identified using BLASTP (Camacho *et al*., 2009) with protein-coding CDS of '*Ca.* M. limnetica' as queries and all protein-coding CDS of '*Ca.* M. limnetica' as subject database. The homologs reported in Table 1 represents the top BLASTP hit (by *e*-value and % sequence identity) and were manually inspected to assure that the alignment coverage was sufficient (typically >90%).

Multiple sequence alignment of amino-acid sequences of nitric oxide reductase was done following the previous alignment by Ettwig and colleagues (2012). Sequences were retrieved from GenBank, imported into JalView 2.10.1 (Waterhouse *et al*., 2009) and aligned using ClustalOmega 1.0.2 (Sievers *et al*., 2011) web service implemented in JalView.

Metatranscriptome data analysis

Illumina reads were trimmed using Trimmomatic 0.32 (Bolger *et al*., 2014) performing removal of Illumina adapters (ILLUMINACLIP:TruSeq3-SE.fa:2:30:10), adaptive trimming (MAXINFO:100:0.2) and retaining reads with a minimum length of 75 bp (MINLEN:75). Ribosomal RNA reads were removed from the trimmed reads using SortMeRNA 2.1 (Kopylova *et al*., 2012) and the prepackaged 8 rRNA databases (silva-bac-16s-id90, silva-arc-id95, silva-euk-18s-id95, silva-bac-23s-id98, silva-arc-23s-id98, silva-euk-28s-id98, rfam-5s-id98, rfam-5.8s-id98). The non-rRNA reads were mapped to the genome of '*Ca.* M. limnetica' using Bowtie2 2.1.0 (Langmead and Salzberg, 2012) and standard parameters. Indexed BAM files were generated using samtools 0.1.19 (Li *et al*., 2009) and the count of alignment to genomic features (based on the indexed BAM file as well as GFF file generated by Prokka) was performed using bedtools 2.23.0 multicov tool (Quinlan and Hall, 2010). Normalized gene transcription was quantified as 'reads per kilobase and million' [RPKM, (Mortazavi *et al*., 2008)] which was calculated by counting the number of mapping reads per gene divided by gene length (in kilobases) and sum of reads mapping to all genes (in millions).

Phylogenetic analyses

Full length 16S rRNA gene sequence was retrieved from the genome of '*Ca.* M. limnetica' using RNAmmer 1.2 (Lagesen *et al*., 2007), aligned using the SILVA incremental aligner (SINA) (Pruesse *et al*., 2012) and imported

to the SILVA SSU NR99 database [release 123; (Quast *et al*., 2013)] using ARB 6.1 (Ludwig *et al*., 2004). Additional NC10 16S rRNA gene sequences originating from Lake Constance (Deutzmann and Schink, 2011), Brunssummerheide (Zhu *et al*., 2012) and the Eastern Tropical North Pacific (Padilla *et al*., 2016) were also added to this dataset. Maximum likelihood phylogenetic trees of 16S rRNA gene sequences were calculated using RAxML 7.7.2 (Stamatakis, 2006) integrated in ARB with the GAMMA model of rate heterogeneity and the GTR substitution model with 500 bootstraps.

NC10 PmoA amino-acid sequences were identified and retrieved from NCBI GenBank using blastp against the NCBI non-redundant protein database with the PmoA amino-acid sequence of '*Ca.* M limnetica' as query. As an outgroup, methane and ammonia monooxygenase subunit A sequences of *Methylomicrobium japanense* (PmoA, BAE86885.1), *Methylocystis* sp. SC2 (PmoA, CCJ08278.1), *Methylacidiphilum fumariolicum* SolV (PmoA1, CCG92750.1) and *Nitrosomonas cryotolerans* (AmoA, AAG60667.1) were added to the dataset. Maximum likelihood phylogenetic trees were calculated using RAxML 8.2.6 (Stamatakis, 2014) using the GAMMA model of rate heterogeneity and the substitution matrix and base frequency of the WAG model with 100 bootstraps (parameters: -f a -k -N -m PROTGAMMAWAG). Phylogenetic trees were visualized using the Interactive Tree of life (iTOL v3) webservice (Letunic and Bork, 2016).

For analysis of 16S rRNA and rDNA amplicon sequencing (only 2015 samples), forward and reverse read were trimmed with usearch [v9.0.2132, (Edgar, 2010)] to 290nt and 280nt, respectively, merged using FLASH v1.2.11 [min. overlap 15nt, max. overlap 200nt and max. mismatch density 0.4; (Magoč and Salzberg, 2011)] and primers were trimmed using cutadapt [v1.5, (Martin, 2011)]. During quality filtering with PRINSEQ-lite [0.20.4, (Schmieder and Edwards, 2011)] only reads with a length between 400 bp and 430 bp and a mean quality value greater 15 were retained. UPARSE (Edgar, 2013) was used to cluster OTUs (operational taxonomic unit) with read-chimera removal and reads were mapped to the OTUs at a 97% similarity cut-off. Taxonomic classification was done with usearch – UTAX based on the greengenes database (DeSantis *et al*., 2006).

Acknowledgements

We are grateful to the Swiss Federal Institute of Aquatic Science and Technology for the use of its boat, housing and research facilities. We thank Wessam Neweshy and Gabriele Klockgether for technical support, Soeren Ahmerkamp for help with flux calculations and Boran Kartal for helpful discussions. We further thank Matthias Zimmermann and Karin Beck for help in the field and in the laboratory, Patrick Kathriner for nutrient analysis and Helmut Bürgmann for support and helpful discussions. This study was financially supported by the Max-Planck-Gesellschaft, the Deutsche Forschungsgemeinschaft (through the MARUM Center for Marine Environmental Sciences) and the Swiss National Science Foundation (SNF grant no. 135299, 153091, 128707 and CR23I3_156759).

References

Alikhan, N.-F., Petty, N.K., Zakour, N.L.B., and Beatson, S. A. (2011) BLAST Ring Image Generator (BRIG): simple prokaryote genome comparisons. *BMC Genomics* **12**: 402.

Aziz, R.K., Bartels, D., Best, A.A., DeJongh, M., Disz, T., and Edwards, R.A. (2008) The RAST Server: rapid annotations using subsystems technology. *BMC Genomics* **9**: 75.

Bankevich, A., Nurk, S., Antipov, D., Gurevich, A.A., Dvorkin, M., Kulikov, A.S., *et al*. (2012) SPAdes: a new genome assembly algorithm and its applications to single-cell sequencing. *J Comput Biol* **19**: 455–477.

Bastviken, D., Cole, J., Pace, M., and Tranvik, L. (2004) Methane emissions from lakes: dependence of lake characteristics, two regional assessments, and a global estimate. *Global Biogeochem Cycles* **18**: GB4009.

Bergmann, D.J., Zahn, J.A., Hooper, A.B., and DiSpirito, A. A. (1998) Cytochrome P460 Genes from the methanotroph *Methylococcus capsulatus* Bath. *J Bacteriol* **180**: 6440–6445.

Berthold, D.A., and Stenmark, P. (2003) Membrane-bound diiron carboxylate proteins. *Annu Rev Plant Biol* **54**: 497–517.

Bhattacharjee, A.S., Motlagh, A.M., Jetten, M.S., and Goel, R. (2016) Methane dependent denitrification-from ecosystem to laboratory-scale enrichment for engineering applications. *Water Res* **99**: 244–252.

Blees, J., Niemann, H., Wenk, C.B., Zopfi, J., Schubert, C.J., Kirf, M.K., *et al*. (2014) Micro-aerobic bacterial methane oxidation in the chemocline and anoxic water column of deep south-Alpine Lake Lugano (Switzerland). *Limnol Oceanogr* **59**: 311–324.

Blower, T.R., Salmond, G.P., and Luisi, B.F. (2011) Balancing at survival's edge: the structure and adaptive benefits of prokaryotic toxin–antitoxin partners. *Curr Opin Struct Biol* **21**: 109–118.

Bolger, A.M., Lohse, M., and Usadel, B. (2014) Trimmomatic: a flexible trimmer for Illumina sequence data. *Bioinformatics* **30**: 2114–2120.

Bowman, J.P. (2006) The methanotrophs - the families Methylococcaceae and Methylocystaceae. In *The Prokaryotes*. Balows A.T., Trüper H.G., Dworkin M., Harder W., Schleifer K.H. (eds). Springer: Berlin, Heidelberg, Germany; New York, NY, USA, pp. 266–289.

Braman, R.S., and Hendrix, S.A. (1989) Nanogram nitrite and nitrate determination in environmental and biological materials by vanadium (III) reduction with chemiluminescence detection. *Anal Chem* **61**: 2715–2718.

Buchfink, B., Xie, C., and Huson, D.H. (2015) Fast and sensitive protein alignment using DIAMOND. *Nat Methods* **12**: 59–60.

Bushnell, B. (2016). BBMap short read aligner [WWW document]. URL http://sourceforge.net/projects/bbmap.

Buts, L., Lah, J., Dao-Thi, M.-H., Wyns, L., and Loris, R. (2005) Toxin–antitoxin modules as bacterial metabolic stress managers. *Trends Biochem Sci* **30**: 672–679.

Camacho, C., Coulouris, G., Avagyan, V., Ma, N., Papadopoulos, J., Bealer, K., and Madden, T.L. (2009) BLAST+: architecture and applications. *BMC Bioinformatics* **10**: 421.

Campbell, M.A., Nyerges, G., Kozlowski, J.A., Poret-Peterson, A.T., Stein, L.Y., and Klotz, M.G. (2011) Model of the molecular basis for hydroxylamine oxidation and nitrous oxide production in methanotrophic bacteria. *FEMS Microbiol Lett* **322**: 82.

DeSantis, T.Z., Hugenholtz, P., Larsen, N., Rojas, M., Brodie, E.L., Keller, K., *et al*. (2006) Greengenes, a chimera-checked 16S rRNA gene database and workbench compatible with ARB. *Appl Environ Microbiol* **72**: 5069–5072.

Deutzmann, J.S., and Schink, B. (2011) Anaerobic oxidation of methane in sediments of Lake Constance, an oligotrophic freshwater lake. *Appl Environ Microbiol* **77**: 4429–4436.

Deutzmann, J.S., Stief, P., Brandes, J., and Schink, B. (2014) Anaerobic methane oxidation coupled to denitrification is the dominant methane sink in a deep lake. *Proc Natl Acad Sci USA* **111**: 18273–18278.

Dibrova, D.V., Cherepanov, D.A., Galperin, M.Y., Skulachev, V.P., and Mulkidjanian, A.Y. (2013) Evolution of cytochrome bc complexes: from membrane-anchored dehydrogenases of ancient bacteria to triggers of apoptosis in vertebrates. *Biochim Biophys Acta* **1827**: 1407–1427.

Dibrova, D.V., Shalaeva, D.N., Galperin, M.Y., and Mulkidjanian, A.Y. (2017) Emergence of cytochrome bc complexes in the context of photosynthesis. *Physiol Plant* **161**: 150–170.

Dupont, C.L., Rusch, D.B., Yooseph, S., Lombardo, M.-J., Richter, R.A., Valas, R., *et al*. (2012) Genomic insights to SAR86, an abundant and uncultivated marine bacterial lineage. *ISME J* **6**: 1186–1199.

Edgar, R.C. (2010) Search and clustering orders of magnitude faster than BLAST. *Bioinformatics* **26**: 2460–2461.

Edgar, R.C. (2013) UPARSE: highly accurate OTU sequences from microbial amplicon reads. *Nat Methods* **10**: 996–998.

Ettwig, K.F., Butler, M.K., Le Paslier, D., Pelletier, E., Mangenot, S., Kuypers, M.M., *et al*. (2010) Nitrite-driven anaerobic methane oxidation by oxygenic bacteria. *Nature* **464**: 543–548.

Ettwig, K.F., Speth, D.R., Reimann, J., Wu, M.L., Jetten, M. S., and Keltjens, J.T. (2012) Bacterial oxygen production in the dark. *Front Microbiol* **3**: 273.

Ettwig, K.F., Zhu, B., Speth, D., Keltjens, J.T., Jetten, M.S., and Kartal, B. (2016) Archaea catalyze iron-dependent anaerobic oxidation of methane. *Proc Natl Acad Sci USA* **113**: 12792–12796.

Goris, J., Konstantinidis, K.T., Klappenbach, J.A., Coenye, T., Vandamme, P., and Tiedje, J.M. (2007) DNA–DNA hybridization values and their relationship to whole-genome sequence similarities. *Int J Syst Evol Microbiol* **57**: 81–91.

Haroon, M.F., Hu, S., Shi, Y., Imelfort, M., Keller, J., Hugenholtz, P., *et al*. (2013) Anaerobic oxidation of methane coupled to nitrate reduction in a novel archaeal lineage. *Nature* **500**: 567–570.

Hayes, C.S., and Low, D.A. (2009) Signals of growth regulation in bacteria. *Curr Opin Microbiol* **12**: 667–673.

He, Z., Cai, C., Wang, J., Xu, X., Zheng, P., Jetten, M.S., and Hu, B. (2016) A novel denitrifying methanotroph of the NC10 phylum and its microcolony. *Sci Rep* **6**: 32241.

Hein, S., Witt, S., and Simon, J. (2017) Clade II nitrous oxide respiration of Wolinella succinogenes depends on the NosG,-C1,-C2,-H electron transport module, NosB and a Rieske/cytochrome bc complex. *Environ Microbiol* **19**: 4913–4925.

Holmes, R.M., Aminot, A., Kérouel, R., Hooker, B.A., and Peterson, B.J. (1999) A simple and precise method for measuring ammonium in marine and freshwater ecosystems. *Can J Fish Aquat Sci* **56**: 1801–1808.

Hügler, M., and Sievert, S.M. (2011) Beyond the Calvin cycle: autotrophic carbon fixation in the ocean. *Annu Rev Mar Sci* **3**: 261–289.

Hyatt, D., Chen, G.-L., LoCascio, P.F., Land, M.L., Larimer, F.W., and Hauser, L.J. (2010) Prodigal: prokaryotic gene recognition and translation initiation site identification. *BMC Bioinformatics* **11**: 119.

Kalyuzhnaya, M.G., Yang, S., Rozova, O., Smalley, N., Clubb, J., Lamb, A., *et al*. (2013) Highly efficient methane biocatalysis revealed in a methanotrophic bacterium. *Nat Commun* **4**: 2785.

Karst, S.M., Kirkegaard, R.H., and Albertsen, M. (2016) *mmgenome: A Toolbox for Reproducible Genome Extraction from Metagenomes*. *bioRxiv*, https://doi.org/10.1101/059121.

Kits, K.D., Klotz, M.G., and Stein, L.Y. (2015a) Methane oxidation coupled to nitrate reduction under hypoxia by the Gammaproteobacterium *Methylomonas denitrificans*, sp. nov. type strain FJG1. *Environ Microbiol* **17**: 3219–3232.

Kits, K.D., Campbell, D.J., Rosana, A.R., and Stein, L.Y. (2015b) Diverse electron sources support denitrification under hypoxia in the obligate methanotroph *Methylomicrobium album* strain BG8. *Front Microbiol* **6**: 1072.

Klindworth, A., Pruesse, E., Schweer, T., Peplies, J., Quast, C., Horn, M., and Glöckner, F.O. (2013) Evaluation of general 16S ribosomal RNA gene PCR primers for classical and next-generation sequencing-based diversity studies. *Nucleic Acids Res* **41**: e1–e1.

Knittel, K., and Boetius, A. (2009) Anaerobic oxidation of methane: progress with an unknown process. *Annu Rev Microbiol* **63**: 311–334.

Kojima, H., Tsutsumi, M., Ishikawa, K., Iwata, T., Mußmann, M., and Fukui, M. (2012) Distribution of putative denitrifying methane oxidizing bacteria in sediment of a freshwater lake, Lake Biwa. *Syst Appl Microbiol* **35**: 233–238.

Kojima, H., Tokizawa, R., Kogure, K., Kobayashi, Y., Itoh, M., Shiah, F.-K., *et al*. (2014) Community structure of planktonic methane-oxidizing bacteria in a subtropical reservoir characterized by dominance of phylotype closely related to nitrite reducer. *Sci Rep* **4**: 5728.

Konstantinidis, K.T., Rosselló-Móra, R., and Amann, R. (2017) Uncultivated microbes in need of their own taxonomy. *ISME J* **11**: 2399–2406.

Kopylova, E., Noé, L., and Touzet, H. (2012) SortMeRNA: fast and accurate filtering of ribosomal RNAs in metatranscriptomic data. *Bioinformatics* **28**: 3211–3217.

Lagesen, K., Hallin, P., Rødland, E.A., Stærfeldt, H.-H., Rognes, T., and Ussery, D.W. (2007) RNAmmer: consistent and rapid annotation of ribosomal RNA genes. *Nucleic Acids Res* **35**: 3100–3108.

Langmead, B., and Salzberg, S.L. (2012) Fast gapped-read alignment with Bowtie 2. *Nat Methods* **9**: 357–359.

Letunic, I., and Bork, P. (2016) Interactive tree of life (iTOL) v3: an online tool for the display and annotation of phylogenetic and other trees. *Nucleic Acids Res* **44**: W242–W245.

Li, H., Handsaker, B., Wysoker, A., Fennell, T., Ruan, J., Homer, N., *et al*. (2009) The sequence alignment/map format and SAMtools. *Bioinformatics* **25**: 2078–2079.

López-Archilla, A.I., Moreira, D., Velasco, S., and López-García, P. (2007) Archaeal and bacterial community composition of a pristine coastal aquifer in Donana National Park, Spain. *Aquat Microbial Ecol* **47**: 123–139.

Ludwig, W., Strunk, O., Westram, R., Richter, L., Meier, H., Buchner, A. *et al*. (2004) ARB: a software environment for sequence data. *Nucleic Acids Res* **32**: 1363–1371.

Luesken, F.A., Sánchez, J., Van Alen, T.A., Sanabria, J., den Camp, H.J.O., Jetten, M.S., and Kartal, B. (2011a) Simultaneous nitrite-dependent anaerobic methane and ammonium oxidation processes. *Appl Environ Microbiol* **77**: 6802–6807.

Luesken, F.A., van Alen, T.A., van der Biezen, E., Frijters, C., Toonen, G., Kampman, C., *et al*. (2011b) Diversity and enrichment of nitrite-dependent anaerobic methane oxidizing bacteria from wastewater sludge. *Appl Microbiol Biotechnol* **92**: 845–854.

Luesken, F.A., Wu, M.L., Op den Camp, H.J., Keltjens, J.T., Stunnenberg, H., Francoijs, K.-J., *et al*. (2012) Effect of oxygen on the anaerobic methanotroph '*Candidatus* Methylomirabilis oxyfera': kinetic and transcriptional analysis. *Environ Microbiol* **14**: 1024–1034.

Magoč, T., and Salzberg, S.L. (2011) FLASH: fast length adjustment of short reads to improve genome assemblies. *Bioinformatics* **27**: 2957–2963.

Martin, M. (2011) Cutadapt removes adapter sequences from high-throughput sequencing reads. *EMBnetjournal* **17**: 10–12.

Milucka, J., Kirf, M., Lu, L., Krupke, A., Lam, P., Littmann, S., *et al*. (2015) Methane oxidation coupled to oxygenic photosynthesis in anoxic waters. *ISME J* **9**: 1991–2002.

Mortazavi, A., Williams, B.A., McCue, K., Schaeffer, L., and Wold, B. (2008) Mapping and quantifying mammalian transcriptomes by RNA-Seq. *Nat Methods* **5**: 621–628.

Müller, B. (1993) Sauerstoffentwicklung im Zugersee. Master's Thesis. Zürich, Switzerland: ETH Zürich.

Nurk, S., Meleshko, D., Korobeynikov, A., and Pevzner, P. (2017) metaSPAdes: A New Versatile De Novo Metagenomics Assembler. *Genome Res* **27**: 824–834.

Nyerges, G., and Stein, L.Y. (2009) Ammonia cometabolism and product inhibition vary considerably among species of methanotrophic bacteria. *FEMS Microbiol Lett* **297**: 131–136.

Op den Camp, H.J., Islam, T., Stott, M.B., Harhangi, H.R., Hynes, A., Schouten, S., *et al*. (2009) Environmental, genomic and taxonomic perspectives on methanotrophic Verrucomicrobia. *Environ Microbiol Rep* **1**: 293–306.

Oremland, R.S., and Culbertson, C.W. (1992) Importance of methane-oxidizing bacteria in the methane budget as revealed by the use of a specific inhibitor. *Nature* **356**: 421–423.

Oswald, K., Milucka, J., Brand, A., Hach, P., Littmann, S., Wehrli, B., *et al*. (2016) Aerobic gammaproteobacterial methanotrophs mitigate methane emissions from oxic and anoxic lake waters. *Limnol Oceanogr* **61**: S101–S118.

Oswald, K., Graf, J.S., Littmann, S., Tienken, D., Brand, A., Wehrli, B., *et al*. (2017) Crenothrix are major methane consumers in stratified lakes. *ISME J* **11**: 2124–2140.

Padilla, C.C., Bristow, L.A., Sarode, N., Garcia-Robledo, E., Ramírez, E.G., Benson, C.R., *et al*. (2016) NC10 bacteria in marine oxygen minimum zones. *ISME J* **10**: 2067–2071.

Padilla, C.C., Bertagnolli, A.D., Bristow, L.A., Sarode, N., Glass, J.B., Thamdrup, B., and Stewart, F.J. (2017) Metagenomic binning recovers a transcriptionally active Gammaproteobacterium linking methanotrophy to partial denitrification in an anoxic oxygen minimum zone. *Front Mar Sci* **4**: 23.

Parks, D.H., Imelfort, M., Skennerton, C.T., Hugenholtz, P., and Tyson, G.W. (2015) CheckM: assessing the quality of microbial genomes recovered from isolates, single cells, and metagenomes. *Genome Res* **25**: 1043–1055.

Parsons, T.R., Maita, Y., and Lalli, C.M. (1984) *A Manual of Biological and Chemical Methods for Seawater Analysis*. Oxford, UK: Pergamon Press, pp. 14–17.

Pereira, M.M., Santana, M., and Teixeira, M. (2001) A novel scenario for the evolution of haem–copper oxygen reductases. *Biochim Biophys Acta* **1505**: 185–208.

Pernthaler, A., Pernthaler, J., and Amann, R. (2002) Fluorescence in situ hybridization and catalyzed reporter deposition for the identification of marine bacteria. *Appl Environ Microbiol* **68**: 3094–3101.

Powell, T., and Jassby, A. (1974) The estimation of vertical eddy diffusivities below the thermocline in lakes. *Water Resour Res* **10**: 191–198.

Pruesse, E., Peplies, J., and Glöckner, F.O. (2012) SINA: accurate high-throughput multiple sequence alignment of ribosomal RNA genes. *Bioinformatics* **28**: 1823–1829.

Quast, C., Pruesse, E., Yilmaz, P., Gerken, J., Schweer, T., Yarza, P., *et al*. (2013) The SILVA ribosomal RNA gene database project: improved data processing and web-based tools. *Nucleic Acids Res* **41**: D590–D596.

Quinlan, A.R., and Hall, I.M. (2010) BEDTools: a flexible suite of utilities for comparing genomic features. *Bioinformatics* **26**: 841–842.

Raghoebarsing, A.A., Pol, A., Van de Pas-Schoonen, K.T., Smolders, A.J., Ettwig, K.F., Rijpstra, W.I.C., *et al*. (2006) A microbial consortium couples anaerobic methane oxidation to denitrification. *Nature* **440**: 918–921.

Rasigraf, O., Kool, D.M., Jetten, M.S., Damsté, J.S.S., and Ettwig, K.F. (2014) Autotrophic carbon dioxide fixation via the Calvin-Benson-Bassham cycle by the denitrifying methanotroph "*Candidatus* Methylomirabilis oxyfera". *Appl Environ Microbiol* **80**: 2451–2460.

Reeburgh, W.S. (2003) Global methane biogeochemistry. *Treatise Geochem* **4**: 347.

Richter, M., and Rosselló-Móra, R. (2009) Shifting the genomic gold standard for the prokaryotic species definition. *Proc Natl Acad Sci USA* **106**: 19126–19131.

Richter, M., Rosselló-Móra, R., Glöckner, F.O., and Peplies, J. (2016) JSpeciesWS: a web server for prokaryotic species circumscription based on pairwise genome comparison. *Bioinformatics* **32**: 929–931.

Schmieder, R., and Edwards, R. (2011) Quality control and preprocessing of metagenomic datasets. *Bioinformatics* **27**: 863–864.

Schubert, C.J., Vazquez, F., Lösekann-Behrens, T., Knittel, K., Tonolla, M., and Boetius, A. (2011) Evidence for anaerobic oxidation of methane in sediments of a freshwater system (Lago di Cadagno). *FEMS Microbiol Ecol* **76**: 26–38.

Seemann, T. (2014) Prokka: rapid prokaryotic genome annotation. *Bioinformatics* **30**: 2068–2069.

Shen, L-D., Hu, B-L., Liu, S., Chai, X-P., He, Z-F., Ren, H-X., *et al*. (2016) Anaerobic methane oxidation coupled to nitrite reduction can be a potential methane sink in coastal environments. *Appl Microbiol Biotechnol* **100**: 7171–7180.

Sievers, F., Wilm, A., Dineen, D., Gibson, T.J., Karplus, K., Li, W., *et al*. (2011) Fast, scalable generation of high-quality protein multiple sequence alignments using Clustal Omega. *Mol Syst Biol* **7**: 539.

Sinclair, L., Peura, S., Hernandez, P., Schattenhofer, M., and Eiler, A. (2017) Novel Chemolithotrophic and Anoxygenic Phototrophic Genomes Extracted from Ice-Covered Boreal Lakes. *bioRxiv*, https://doi.org/10.1101/139212.

Stamatakis, A. (2006) RAxML-VI-HPC: maximum likelihood-based phylogenetic analyses with thousands of taxa and mixed models. *Bioinformatics* **22**: 2688–2690.

Stamatakis, A. (2014) RAxML version 8: a tool for phylogenetic analysis and post-analysis of large phylogenies. *Bioinformatics* **30**: 1312–1313.

Vaksmaa, A., van Alen, T.A., Ettwig, K.F., Lupotto, E., Valè, G., Jetten, M.S., and Lüke, C. (2017) Stratification of diversity and activity of methanogenic and methanotrophic microorganisms in a nitrogen-fertilized Italian paddy soil. *Front Microbiol* **8**: 2127.

Waterhouse, A.M., Procter, J.B., Martin, D.M., Clamp, M., and Barton, G.J. (2009) Jalview Version 2—a multiple sequence alignment editor and analysis workbench. *Bioinformatics* **25**: 1189–1191.

Weber, H.S., Habicht, K.S., and Thamdrup, B. (2017) Anaerobic methanotrophic archaea of the ANME-2d cluster are active in a low-sulfate, iron-rich freshwater sediment. *Front Microbiol* **8**: 619.

Wiesenburg, D.A., and Guinasso, N.L. (1979) Equilibrium solubilities of methane, carbon monoxide, and hydrogen in water and sea water. *J Chem Eng Data* **24**: 356–360.

Wu, M.L., Ettwig, K.F., Jetten, M.S., Strous, M., Keltjens, J. T., and van Niftrik, L. (2011a) A new intra-aerobic metabolism in the nitrite-dependent anaerobic methane-oxidizing bacterium *Candidatus* 'Methylomirabilis oxyfera'. *Biochem Soc Trans* **39**: 243–248.

Wu, M.L., de Vries, S., van Alen, T.A., Butler, M.K., Op den Camp, H.J.M., Keltjens, J.T., *et al*. (2011b) Physiological role of the respiratory quinol oxidase in the anaerobic nitrite-reducing methanotroph '*Candidatus* Methylomirabilis oxyfera'. *Microbiology* **157**: 890–898.

Yarza, P., Yilmaz, P., Pruesse, E., Glöckner, F.O., Ludwig, W., Schleifer, K.-H., *et al*. (2014) Uniting the classification of cultured and uncultured bacteria and archaea using 16S rRNA gene sequences. *Nat Rev Microbiol* **12**: 635–645.

Zhu, B., van Dijk, G., Fritz, C., Smolders, A.J., Pol, A., Jetten, M.S., and Ettwig, K.F. (2012) Anaerobic oxidization of methane in a minerotrophic peatland: enrichment of nitrite-dependent methane-oxidizing bacteria. *Appl Environ Microbiol* **78**: 8657–8665.

Supporting Information

Additional Supporting Information may be found in the online version of this article at the publisher's web-site:

Fig. 1. Physico-chemical parameters and abundance of NC10 bacteria in Lake Zug in October 2015. (a) Depth concentration profile of oxygen and methane throughout the water column (methane only 100–140 m). (b) Concentration profiles of NO_x (nitrate + nitrite) and ammonium. The grey bars (100–140 m) show relative abundance of NC10 bacteria as determined by 16S rRNA gene amplicon sequencing.

Fig. 2. Differential coverage plot of the co-assembled metagenomes from Lake Zug. "*Ca.* M. limnetica" genomic bin (outlined) was extracted from the metagenomic contigs of the Lake Zug co-assembly by exploiting differential coverage binning. Each contig is represented by a circle and the circle size reflects contig length (in Kbp). Colored circles show taxonomic assignment of essential single copy genes; "*Ca.* M. limnetica" contigs were classified as unclassified bacteria.

Fig. 3. "*Ca.* Methylomirabilis oxyfera" genome coverage by metagenomic sequences of the Lake Zug 160 m metagenome. Shown is the circular genome of "*Ca.* M. oxyfera"; the middle ring shows average-fold genome coverage in blue (0 – 1000x, in 500 bp intervals) by sequences of the metagenome from 160 m depth. Genomic localization of selected functional genes of "*Ca.* M. oxyfera" involved in oxygen and nitrogen respiration as well as carbon metabolism are shown on the outer and inner ring as black intervals. Locus tags of the respective genes are shown in brackets; gene names in bold typeface were not identified in the genome of "*Ca.* M. limnetica".

Fig. 4. Organization of gene clusters encoding for cytochrome *bc*-like complexes of "*Ca.* M. limnetica". Gene clusters of cytochrome *bc*-like complexes of "*Ca.* M. limnetica" (CLG94_00765-00785, CLG94_01010-01025) as well as a third complex exclusive to "*Ca.* M. oxyfera"

(DAMO_00767-69) is shown. Position of domains/motifs and gene product length are drawn to scale (aa: amino acids) and motifs are specified in the Figure. Protein domains were identified using NCBI conserved domains database (Marchler-Bauer *et al.*, 2016) or manually (using CxxCH motif for *c*-type hemes); transmembrane helices were identified using the TMHMM Server 2.0 (http://www.cbs.dtu.dk/services/TMHMM/; Krogh *et al*., 2001) Abbreviations: TMH, transmembrane helix; 2Fe-2S, Rieske iron-sulfur cluster.

Fig. 5. Multiple alignment of nitric oxide reductase (qNOR) and putative nitric oxide dismutase (NOD). Quinol-binding site and catalytic site are shown for nitric oxide reductase (red) and putative nitric oxide dismutase (blue) following the previous alignment by Ettwig *et al*. (2012); the numbering is according to the residue number of *G. stearothermophilus.* Accession numbers: *Geobacillus stearothermophilus* 3AYF_A, *Neisseria gonorrhoeae* ZP_04723508.1, *Synechocystis* sp. PCC 6803 BAA18795.1, gamma proteobacterium HdN1 NorZ1 (CBL45628.1) NorZ2 (YP_003809511.1), *Staphylococcus aureus* EGL94648.1, *Muricauda ruestringensis* G2PJH6.

Table 1. Overview of used oligonucleotide probes specific to NC10 bacteria. Listed are target group, 5'-3' sequence, % [v/v] formamide in the hybridization buffer and respective reference.

Table 2. Summary of raw metagenomic and metatranscriptomic sequence data obtained in this study. All water samples for DNA and RNA extraction were taken at the same location.

Table 3. Overview of genome statistics for "*Ca.* M. limnetica" and comparison to "*Ca.* M. oxyfera". The complete genome of "*Ca.* M. oxyfera" was retrieved from GenBank (accession number FP565575.1). Coding sequences, rRNAs and tRNAs were predicted using Prodigal (Hyatt *et al*., 2010), Aragorn (Laslett and Canback, 2004) and RNAmmer (Lagesen *et al*., 2007) implemented in the Prokka annotation pipeline (Seemann, 2014). Genome quality metrics were computed using CheckM (Parks *et al*., 2015) running the lineage specific workflow.

Table 4. Overview of genes encoding for enzymes involved in nitrogen oxide and oxygen respiration of "*Ca.* M. limnetica" and "*Ca.* M. oxyfera". The nomenclature of heme-copper oxidase 1-3 of "*Ca.* M. oxyfera" is listed according to Wu *et al*. (2011).

Table 5. *In situ* transcription of functional genes of "*Ca.* M. limnetica" involved autotrophic CO_2 fixation. Listed are functional genes encoding for autotrophic CO_2 fixation via Calvin-Benson-Bassham pathway. Transcription was quantified as RPKM (reads per 1 kb gene length and per million mapped transcripts) in metatranscriptomes obtained from 110 m, 120 m and 160 m depth.